Folate-bearing doxorubicin-loaded magnetic poly(*N*-isopropylacrylamide) microspheres as a new strategy for cancer therapy

Yong Sun[a], Libo Chen[b], Jerry Yu[a,c], Xiuling Zhi[a], Shaoxian Tang[a], Ping Zhou[a] and Changchun Wang[b]

Doxorubicin is a classic anticancer agent. Recently, numerous strategies have been used to enhance efficacy of drug delivery for cancer treatment. For example, by modifying poly(*N*-isopropylacrylamide) microspheres, a nanocarrier, makes it more effective. Conjugation with folic acid increases specific targeted drug delivery towards folate receptor-bearing cancer cells to improve anticancer effectiveness by increasing the tissue's local concentration of drugs. In the current studies, we synthesized folate-bearing, doxorubicin-loaded, magnetic, poly-(*N*-isopropylacrylamide) microspheres (FDMPM) to treat breast cancer cells (human SKBR-3). We found efficiency of drug encapsulation very high (95%) at pH above 7.4. Reverse transcription-PCR showed that cancer cells highly expressed folate receptors. Confocal laser scanning microscopy and flow cytometry revealed internalization of the carrier by SKBR-3 in treatments with FDMPM, which was not the case with any other combination for drug delivery (MPM, FMPM, and DMPM). Similarly, SKBR-3 cell growth was inhibited more (assessed by methylthiazolyl-diphenyl-tetrazolium bromide and trypan blue exclusion assays) when treated with FDMPM than with any other combinations. Current results confirm our predication and demonstrate that FDMPM has potential as a new targeting strategy in cancer therapy. ***Anti-Cancer Drugs*** **20:607–615 © 2009 Wolters Kluwer Health | Lippincott Williams & Wilkins.**

Anti-Cancer Drugs 2009, **20:**607–615

Keywords: anticancer agent, breast cancer, doxorubicin, drug delivery systems, folate, magnetic poly(*N*-isopropylacrylamide) microspheres, nanomedicine

[a]Department of Physiology and Pathophysiology, Shanghai Medical College, [b]Key Laboratory of Molecular Engineering of Polymers (Ministry of Education), Department of Macromolecular Science and Advanced Materials Laboratory, Fudan University, Shanghai, China and [c]Department of Pulmonary Medicine, University of Louisville, Kentucky, USA

Correspondence to Dr Ping Zhou, MD, PhD, Department of Physiology and Pathophysiology, Shanghai Medical College, Fudan, University, 138# Yixueyuan Road, Shanghai 200032, China
Tel: +86 21 54237392; fax: +86 21 64221201; e-mail: zping@shmu.edu.cn
or
Professor Changcun Wang, Key Laboratory of Molecular Engineering of Polymers and Department of Macromolecular Science, Advanced Materials Laboratory, Fudan University, Shanghai 200433, China
Fax: +86 21 6564 0293; e-mail: ccwang@fudan.edu.cn

Yong Sun and Libo Chen contributed equally to this study

Received 16 December 2008 **Revised form accepted** 10 February 2009

Introduction

Quinones are classic drugs about 50 years old and used in cancer treatment [1]. For example, doxorubicin (DOX), an anthracycline antibiotic [2], is used routinely to treat breast and lung cancers [3]. DOX causes DNA damage through topoisomerase II inhibition and free radical generation by redox reaction [4]. Its anticancer effect in the S phase is much more obvious than in the G_0, G_1, G_2, and M phases [5]. Like many anticancer drugs, DOX is intrinsically fluorescent. Thus, its concentration inside cells can be determined by visualization with various microscopic imaging technologies [6].

Polymeric microspheres with a hollow chamber have unique properties such as small size, large inner volume, and variable permeability. Thus, they are ideal for encapsulation of drugs, DNA, enzymes, and other active biomacromolecules [7–10]. Recent research has focused on designing microspheres that can undergo reversible structure changes in response to external stimuli, such as pH, temperature, ion strength, and magnetic field. Poly(*N*-isopropylacrylamide) microspheres (PM) are thermosensitive. Linear poly(*N*-isopropylacrylamide) has a lower critical solution temperature (LCST) at 32°C. PM cross-linked to methylene bisacrylamide exhibits volume phase transition at the LCST and shrinks above the LCST to release its liquid content. The volume phase transition temperature (VPTT) of cross-linked PM can be adjusted by adding a co-monomer. Hydrophilic co-monomers increase the VPTT, whereas hydrophobic ones decrease the VPTT [11]. Owing to its thermosensitive properties, PM is considered a promising candidate for effective drug delivery.

Magnetic nanoparticles have been widely used in biological applications, such as magnetic resonance imaging, tissue-specific releasing of therapeutic agents, sorting of cells, separation of biochemical products, and drug delivery systems [12–14]. Placing magnetic nanoparticles into polymer capsules as a component of the shell, or directly into the chamber would help prevent capsular aggregation in liquids and improve their chemical stability.

0959-4973 © 2009 Wolters Kluwer Health | Lippincott Williams & Wilkins DOI: 10.1097/CAD.0b013e32832a2ef0

The membrane-bound folate receptor (FR) is rarely expressed in normal cells. However, it is overexpressed in many malignant tumors, such as lung, ovary, cervix, endometrium, kidney, mammary gland, brain, and colon carcinomas [15,16]. Folic acid (FA) is a high-affinity ligand of the FR. Its conjugates may still possess receptor-binding properties and be taken up by cancer cells through receptor-mediated endocytosis, thus providing targeted drug delivery to FR-positive cancer cells. Such a folate-bearing delivery system significantly enhances specificity and sensitivity over a folate-devoid one. Owing to its high affinity to FR, folate has been popularly used as a targeting moiety to increase cell uptake of anticancer agents in the forms of polymer microspheres, liposomes, and nanoparticles [17–20]. Usually, folate is covalently conjugated to these agents, and polymeric microspheres are an ideal candidate for targeted drug delivery.

In the current studies, we used PM as a target-specific nanocarrier for DOX. We synthesized folate-bearing, magnetic PM (FMPM), with magnetic Fe_3O_4 nanoparticles as cores and polymers as shells. These microspheres have hollow chambers for loading DOX to form folate-bearing, DOX-loaded, magnetic PM (FDMPM). With responses to both magnetic field and temperature, these multifunctional FDMPM may destroy breast cancer cells effectively.

Experimental methods

Materials

N-isopropylacrylamide and glycidyl methacrylate were purchased from Aldrich (Sigma, St Louis, Missouri, USA). *N*,*N*′-methylenebisacrylamide and iron (II) chloride tetrahydrate ($FeCl_2.4H_2O$) were purchased from Fluka. Iron (III) chloride hexahydrate ($FeCl_3.6H_2O$), folate and oleic acid were purchased from Sinopharm Chemical Reagent Co. Ltd. *N*-hydroxysuccininimide and 1-ethyl-3-(3-dimethylaminopropyl)-carbodiimide–HCl (EDC–HCl) were purchased from Shanghai Med pep Co. Ltd (Shanghai China). Dimethyl sulfoxide, butyl acetate, 1,6-diaminohexane, and sodium dodecyl benzene sulfonate (SDBS) were purchased from Shanghai Chemical Reagent Co. (Shanghai China). KPS was purchased from Shanghai Aijian reactant factory (Shanghai China) and recrystallized from water.

Synthesis of Fe_3O_4 nanoparticles

Preparations of Fe_3O_4 nanoparticle were carried out by a well-established coprecipitation method. Typically, a small amount of oleic acid was added to stabilize Fe_3O_4 during coprecipitation of $FeCl_2$ and $FeCl_3$ in sodium hydroxyl solution under a N_2 atmosphere at 60°C. The dispersion was heated to 90°C and kept for 0.5 h, and then cooled to room temperature with the pH adjusted to 4 with 1 mol/l HCl. Fe_3O_4 nanoparticles were collected magnetically, and washed with deionized water and ethanol several times. Finally, the oleic acid-modified Fe_3O_4 nanoparticles were dispersed in cyclohexane for further use.

Synthesis of magnetic thermosensitive seed

The seed microspheres were prepared in a typical process: nanoparticles of 0.021 g Fe_3O_4 and 60 mg AIBN (2,2′-azobisisobutyronitrile) were dispersed in 1.5 g *n*-butyl acetate. The dispersion was added to a SDBS solution (60 mg SDBS/90 ml H_2O), and then ultrasonicated for 10 min to a uniform latex. Then, 1.05 g *N*-isopropylacrylamide and 0.15 g methylene bisacrylamide (10% cross-link density) dissolved in 30 ml water were loaded into a four-neck flask equipped with stirrer, condenser, thermometer, and N_2 inlet, and the prementioned latex. After bubbling with N_2 for 30 min, the reaction system was heated to 76°C. Polymerization occurred at 76°C for 4 h. The production was separated by magnets and washed with deionized water several times.

Synthesis of magnetic poly(*N*-isopropylacrylamide) microsphere

Typically, 0.064 g *N*-isopropylacrylamide, 0.020 g glycidyl methacrylate (20% of mole in monomers) and 0.010 g methylene bisacrylamide (10% cross-link density) were added to a 25-ml seed dispersion (1 mg/ml). After bubbling with N_2 for 30 min and adding 4 mg KPS, polymerization occurred at 76°C for 4 h. The production was separated by magnets and washed with de-ionized water.

Synthesis of folate-bearing, magnetic poly(*N*-isopropylacrylamide) microsphere

The presynthesized MPM were redispersed in deionized water, and excess 1,6-diaminohexane was added. The mixture was stirred at 40°C for 20 h, and production with NH_{2-} was separated by magnets and washed with deionized water for further reaction. The FA conjugating reaction was carried out according to an established method. Folate, *N*-hydroxysuccinimide, and EDC–HCl (mole 1 : 2 : 2) were dissolved in dimethyl sulfoxide and reacted for 1 h. The mixture was then added to a NH_{2-} -conjugated microsphere dispersion (the amount of folate was largely excessive to NH_{2-}). After addition of a triethylamine catalyst, the mixture was stirred for 24 h at room temperature for reaction. The solution was separated by magnets and washed with pH 9.18 buffer solution several times. The excess of unreacted folate was removed by dialysis in pH 9.18 buffer solution for 24 h.

In-vitro doxorubicin load and release

Load: DOX–HCl water solution (1 mg/ml) was added to the prepared FMPM (or MPM) water dispersion. The mixture was stirred for 12 h, and the production was separated by centrifugation. Release: the DOX-loaded FMPM (FDMPM) were dispersed in a buffer solution and placed in a dialysis membrane with a molecular weight 5000 Da. The dialysis bag then was immersed in neutralized phthalate buffer (200 ml; pH 6.4) or PBS (200 ml, pH 7.4) at 37°C. Samples of 2 ml were taken at specific time intervals (2 ml buffer solution was supplemented at the same time), and the drug concentration was analyzed

using ultraviolet–visible (UV–vis) spectrophotometry at 485 nm. The drug load and release amounts were calculated based on the standard curve obtained from DOX in the buffers. The method used to calculate the encapsulation efficiency as following:

$$\%\,\text{Drug encapsulation efficiency} = 1 - \frac{\textit{Reliquus}\,\text{DOX in the buffers}}{\text{total DOX}} \times 100\%$$

Characterization

UV–vis absorption spectra were measured on a Perkin Elmer Lambda 35 UV–vis spectrophotometer (Perkin Elmer, Waltham, Massachusetts, USA). One drop of the samples placed on copper grids coated with carbon was examined and the image was obtained with a JEOL-1230 transmission electron microscope (JEOL, Japan). TGA measurements were carried out on a PerkinElmer Pyris-1 series thermal analysis system under a flowing nitrogen atmosphere at a scan rate of 20°C/min from 100 to 600°C. The hydrodynamic diameter of the particles was determined by quasielastic light scattering (Malvern Autosizer 4700; Malvern, UK). A vibrating-sample magnetometer (EG&G Princeton Applied Research, USA; model 155) was used at 305K to measure the magnetic moment.

Gene identification

Total RNA was isolated from the cells using Trizol reagent (Invitrogen, Carlsbad, California, USA) and reverse transcription (RT)-PCR was performed using Superscript II RT (Invitrogen) according to the manufacturer's instructions. Primers for FR gene expression detection were 5′-AGGACTGTGAGCAATGGTGG-3′ (forward) and reverse: 5′-GCGCACTTGTTAAACCCTGAA-3′ (reverse). Primers for β-actin were 5′-AACAGTCCGCCTAGAAGCAC-3′ (forward) and 5′-CGTTGACATCCG TAAAGACC-3′ (reverse). The amplified products were 100 and 281 bp, respectively.

Cell culture and incubation with magnetic poly(*N*-isopropylacrylamide) microspheres

Human SKBR-3 breast cancer cells (MPM; ATCC, Germantown, Maryland, USA) were incubated in Dulbecco's modified Eagle's medium supplemented with 5000 U/ml penicillin, 50 μg/ml streptomycin, and 10% fetal bovine serum at 37°C with 5% CO_2 in 96 flat-bottom wells for 48 h before experiments. After cells had successfully attached to the bottom of the well (normal morphology), MPM, FMPM, DMPM, and FDMPM were added, respectively, to the wells and incubated at 37°C for 4 h.

Localization of magnetic poly(*N*-isopropylacrylamide) microspheres in breast cancer cells

Localization of MPMs was studied with a confocal laser-scanning microscope using 488 nm as excitation light and 585 nm as diverging light to detect DOX (intrinsic fluorescent). Before analysis, the detached SKBR-3 cells were seeded on cover slides in 60 mm cell culture dishes for 48 h. After that, DMPM and FDMPM were added to the dishes at the concentration of 50 μg/ml and incubated at 37°C for 4 h. All confocal measurements were carried out at room temperature (25°C).

Fluorescence intensity of magnetic poly(*N*-isopropylacrylamide) microspheres inside breast cancer cells

Fluorescence intensity of MPMs was studied by flow cytometry using 488 nm as excitation light and 585 nm as diverging light to detect DOX (intrinsic fluorescent), which was loaded in the polymer. Before analysis, the detached SKBR-3 cells were seeded in 12 flat-bottom wells for 48 h. After that, DMPM and FDMPM were added to the wells at different concentrations and incubated at 37°C for 4 h.

Toxicity of the magnetic poly(*N*-isopropylacrylamide) microspheres

Methylthiazolyldiphenyl-tetrazolium bromide (MTT) and trypan blue exclusion assays were used to examine cell proliferation and death. The MTT test uses tetrazolium compound [3-(4,5-dimethylthiazol-2-yl)-5-(3-carboxymethoxyphenyl)-2-(4-sulfophenyl)-2*H*-tetrazolium, inner salt; MTS] and the electron-coupling reagent phenazine methosulfate. MTS is chemically reduced by cells to formazan, which can be measured by optical absorbance at 490 nm, indicating metabolically active cells. At given time intervals, the cultured cells were examined for cell viability with the MTT assay. The wells were washed twice with PBS and then 10 μl of MTT supplemented with 90 μl culture medium was added. After 4 h incubation, the culture medium was removed and the precipitate was dissolved in isopropanol. The absorbance at 490 nm was measured with a microplate reader (Genios, Tecan). Trypan blue, a chemical colorant, is only excluded by live cells. The cell viabilities were measured as following:

$$\%\,\text{Survival rate} = 1 - \frac{\text{blue} - \text{stain cells}}{\text{all cells}} \times 100\%$$

Statistical analysis

All assays were performed at least three times using the *t*-test and statistical significance defined as a P value of less than 0.05.

Results

Structure and properties of folate-bearing, magnetic poly(*N*-isopropylacrylamide) microspheres

Using a soft magnetic template, the prepared magnetic microspheres had clear core-shell structures with hollow chambers. Fe_3O_4 nanoparticles were placed in the chambers as the magnetic cores and the polymers formed the shells (Fig. 1). Each microsphere contained Fe_3O_4

nanoparticles, which were mobile inside the chamber when filled with aqueous solutions but distributed randomly in the cavity when dry. The FMPMs were monodispersed in size with a diameter of about 200 nm as seen with an electron microscope, which made it possible for application in cellular experiments.

With poly(*N*-isopropylacrylamide)-based polymeric shells, the FMPM undergoes a temperature-induced volume phase transition. Poly(*N*-isopropylacrylamide)-based hydrogels have a VPTT around 32°C. In the present studies, using dynamic light scattering, the hydrodynamic diameters of FMPM were found to decrease with increased temperature. Owing to the high cross-linked density (10%), the VPTT of the FMPM, also around 32°C, was not as sharp as the linear polymer. The magnetic property of the FMPM was investigated by a vibrating-sample magnetometer. Fe_3O_4 nanoparticles comprised 67.9% of the weight of the microspheres (measured by thermogravimetric analyzer), and the FMPM we prepared had a very high magnetic saturation of about 40.5 emu/g to meet the requirements in bioapplications. Tagged with folate, our MPM also had special affinity for FRs, which was confirmed by the cell experiments below.

In-vitro loading and releasing of doxorubicin

To investigate the application of the prepared FMPM as drug carriers, we used them to load the anticancer drug DOX (FDMPM). In a typical loading process, the FMPM and DOX (weight 1 : 1) were dispersed in water and stirred overnight. We found that the DOX could be loaded into the FMPM, and drug encapsulation efficiency was pH dependent (Fig. 2). The efficiency increased with increase in pH. It was about 50% at pH 5, and nearly 100% at pH above 8. At pH 7.4, the efficiency of drug encapsulation was about 95%. The solubility of DOX was also pH dependent. DOX became more soluble as pH decreased. Many functional groups, such as amino and hydroxyl groups, in the DOX molecule could have hydrogen bond interactions with MPM. At low pH, DOX was soluble and encapsulated into FMPM, mainly by hydrogen bond interaction. This interaction was weak; therefore, the encapsulation efficiency was relatively low. At higher pH, DOX became insoluble in water and the polymer shells of FMPM captured nearly all the DOX. Thus, encapsulation efficiency was quite high.

Fig. 1

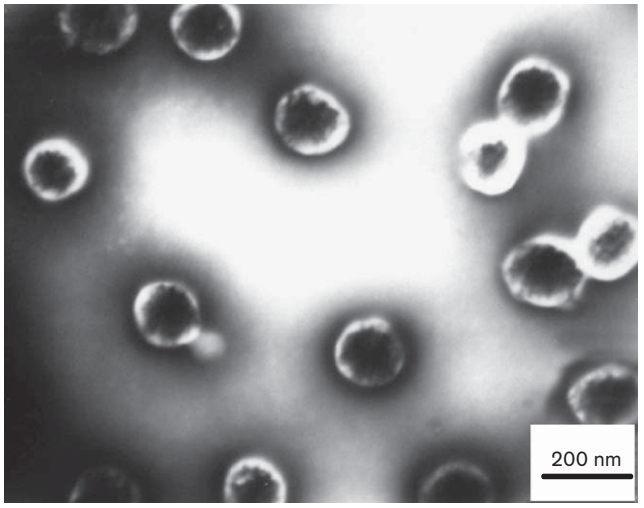

Transmission electron microscopic image of folate-bearing, magnetic poly(*N*-isopropylacrylamide) microsphere. Note that nanoparticles are about 200 nm in diameter.

Fig. 2

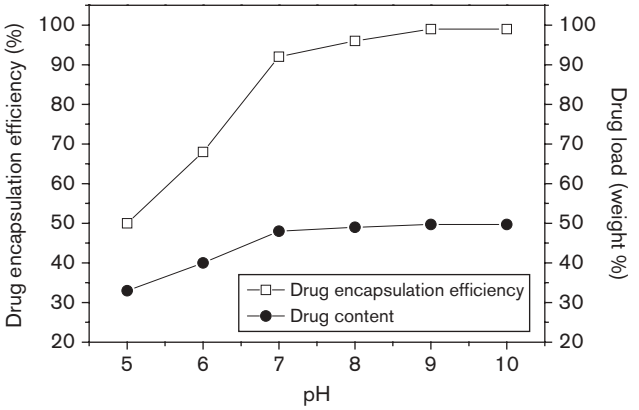

Effects of pH on the doxorubicin encapsulation efficiency and drug load (as weight percentage) that in folate-bearing, magnetic poly(*N*-isopropylacrylamide) microspheres. Note that both encapsulation and drug loading leveled off as pH increased above 7.

Fig. 3

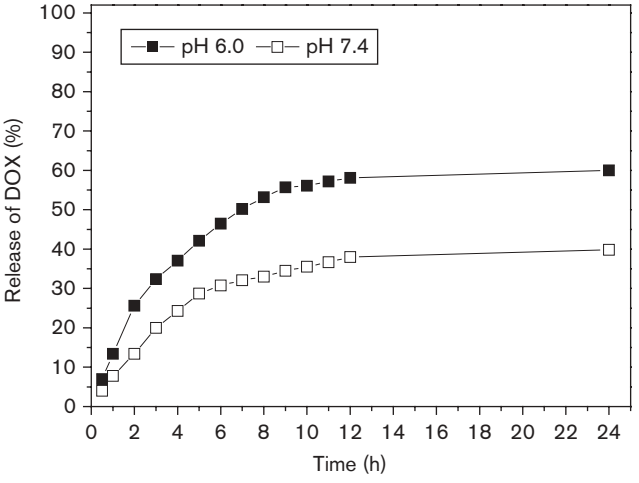

Release of doxorubicin (DOX) from folate-bearing, doxorubicin-loaded, magnetic, poly(*N*-isopropylacrylamide) microspheres at pH 6.0 and 7.4 at 37°C *in vitro*. Drug release reached a plateau after 10 h.

The in-vitro release of DOX from FDMPM was investigated. Figure 3 shows the release profiles of DOX from FDMPM under simulated physiological conditions (PBS, pH 7.4) and an acidic environment (pH 6.0) at 37°C. We chose these conditions because (i) the internal environment of most cancer cells is acidic with a low pH; and (ii) during in-vivo studies (cell experiment), the FDMPM were cultivated at 37°C with tumor cells. Figure 2 shows that DOX was released much faster at pH 6.0 than at pH 7.4, with approximately 60 and 40% of the drug released within 24 h, respectively. It is reasonable to assume that at a low pH, the drug was more soluble and therefore released more rapidly.

Fig. 4

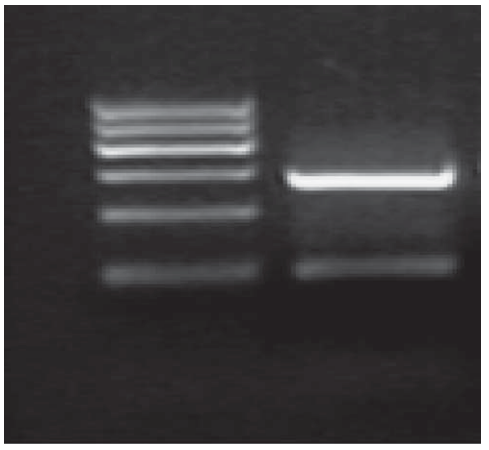

Identification of FR gene expression by RT-PCR. There is an obvious folate receptor (FR) gene band in the lane for SKBR-3.

Gene identification

It has been reported that SKBR-3 breast cancer cells highly express FRs. To confirm this, total RNA from human SKBR-3 breast cancer cells was analyzed by RT-PCR. Figure 4 illustrates the FR band in the lane for SKBR-3.

Localization of magnetic poly(*N*-isopropylacrylamide) microspheres in breast cancer cells

To determine whether the drugs can be effectively delivered into the cancer cells, we assessed the intrinsic fluorescence of DOX [6]. Using light microscopy, non-FA-targeted nanoparticles were located outside cells (Fig. 5a and c), whereas FA-targeted nanoparticles were

Fig. 5

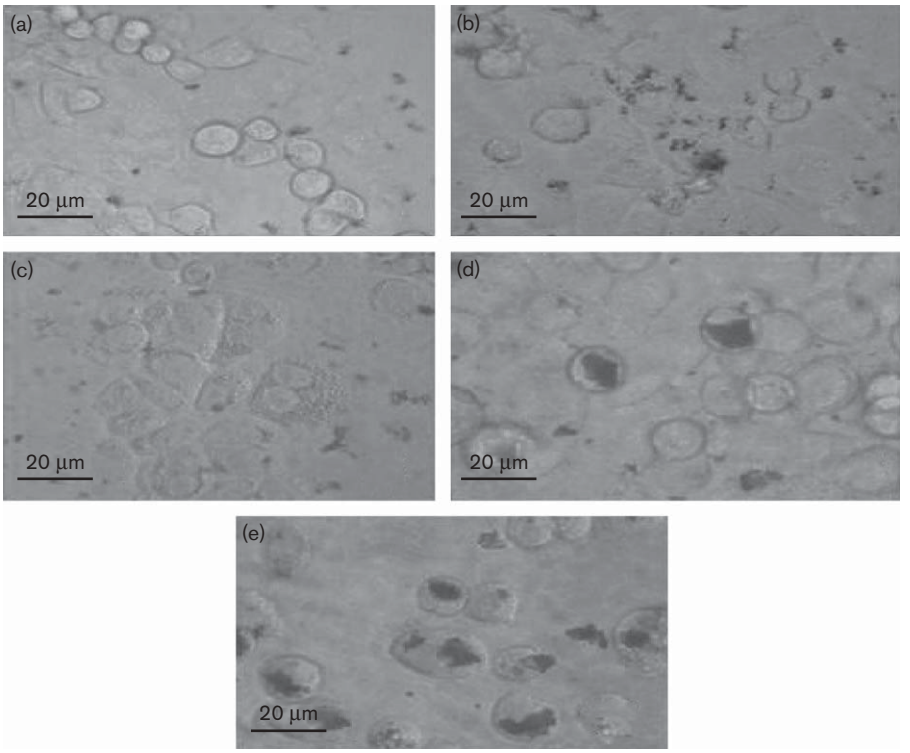

Localization of PNIPAMs microspheres in SKBR-3 breast cancer cells under light microscopy: (a) magnetic poly(*N*-isopropylacrylamide) microspheres; (b) folate-bearing, magnetic poly(*N*-isopropylacrylamide) microspheres; (c) doxorubicin-loaded, magnetic, poly(*N*-isopropylacrylamide) microspheres; (d) folate-bearing, doxorubicin-loaded, magnetic, poly(*N*-isopropylacrylamide) microspheres (FDMPM); (e) the detached cells treated with FDMPM. Non-folic acid (FA)-targeted nanoparticles were located outside cells, whereas FA-targeted nanoparticles were located on the cell surface or inside cells.

located on the cell surface and/or inside cells (Fig. 5b and d). After cells were trypsinized and placed on slides, FDMPM was clearly observed inside SKBR-3 cells (Fig. 5e). Nanoparticles inside cells and the intracellular architecture could be observed under confocal laser scanning microscopy after SKBR-3 cells were incubated with FDMPM (Fig. 6a).

Fig. 6

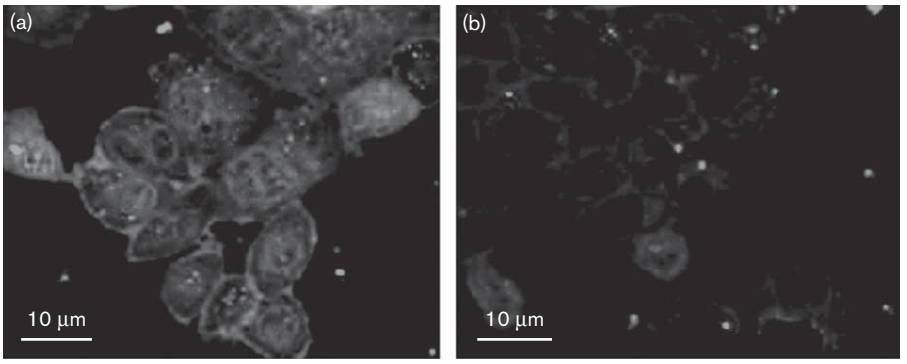

Localization of poly(*N*-isopropylacrylamide) microspheres under confocal microscopy: SKBR-3 breast cancer cells treated with folate-bearing, doxorubicin-loaded, magnetic, poly(*N*-isopropylacrylamide) microspheres (a) or with doxorubicin-loaded, magnetic, poly(*N*-isopropylacrylamide) microspheres (b).

Fig. 7

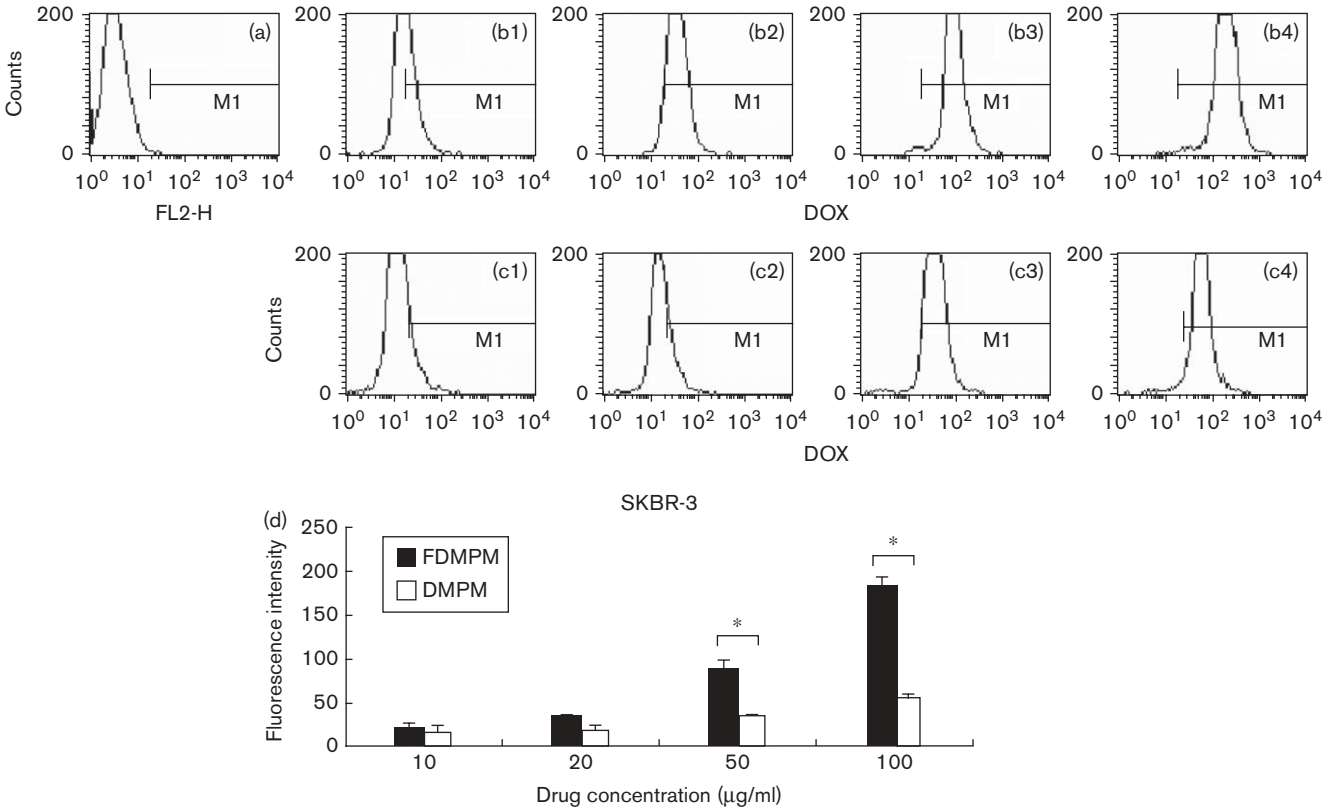

Fluorescence intensity analysis by flow cytometry in SKBR-3 breast cancer cells with different treatments: (a) control; (b) treated with folate-bearing, doxorubicin-loaded, magnetic, poly(*N*-isopropylacrylamide) microspheres (FDMPM) for 4 h at concentrations of: 10 μg/ml (b1); 20 μg/ml (b2); 50 μg/ml (b3); 100 μg/ml (b4); (c) treated with doxorubicin-loaded, magnetic, poly(*N*-isopropylacrylamide) microspheres (DMPM) for 4 h at concentrations of: 10 μg/ml (c1); 20 μg/ml (c2); 50 μg/ml (c3); 100 μg/ml (c4). (d) Mean fluorescence intensity at different drug concentrations. SKBR-3 cells internalize much more FDMPM than DMPM at concentrations of 50 and 100 μg/ml. $*P<0.05$.

Fig. 8

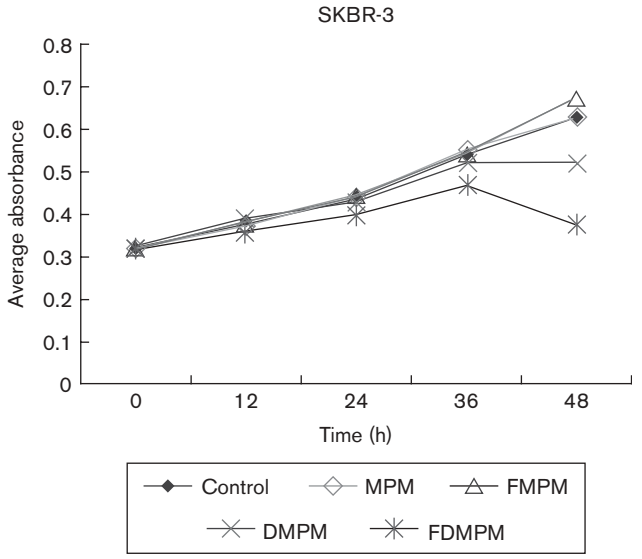

Toxicity assessment by the methylthiazolyldiphenyl-tetrazolium bromide assay. Cell growth in control, magnetic poly(*N*-isopropylacrylamide) microsphere (MPM)-treated and folate-bearing, magnetic poly(*N*-isopropylacrylamide) microsphere (FMPM)-treated groups showed no difference. Cell growths of folate-bearing, doxorubicin-loaded, magnetic, poly(*N*-isopropylacrylamide) microsphere (FDMPM)-treated and doxorubicin-loaded, magnetic, poly(*N*-isopropylacrylamide) microsphere (DMPM)-treated groups are both inhibited. The first group is much more prominent.

Fig. 9

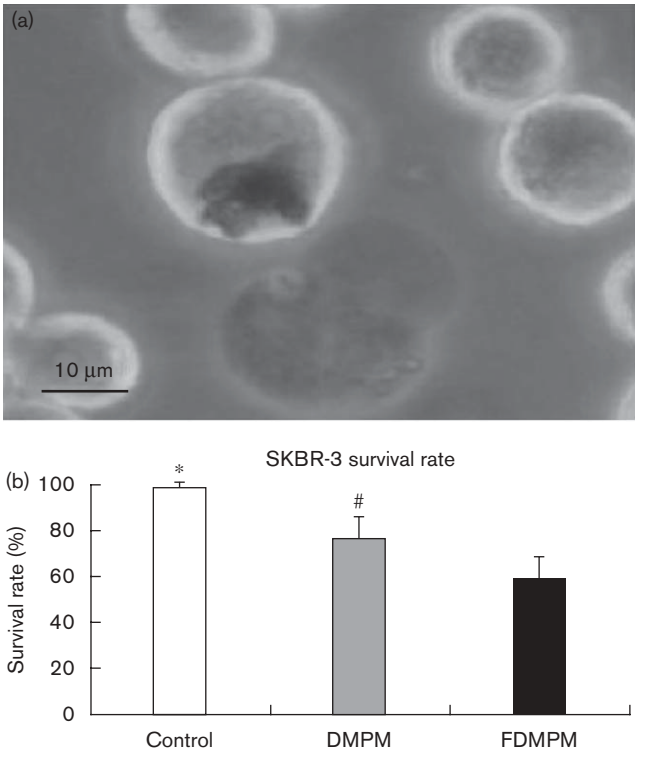

Trypan exclusion assay. (a) SKBR-3 breast cancer cells treated with folate-bearing, doxorubicin-loaded, magnetic, poly(*N*-isopropylacrylamide) microspheres (FDMPM) for 48 h. The cells that are darker indicate cell death. (b) Survival rate of SKBR-3 breast cancer cells incubated with FDMPM for 48 h. $^{*}P<0.05$ vs. doxorubicin-loaded, magnetic, poly(*N*-isopropylacrylamide) microspheres (DMPM) and FDMPM. $^{\#}P<0.05$ vs. FDMPM.

In contrast, when SKBR-3 cells were incubated with DMPM, the cells observed were hollow (Fig. 6b).

Fluorescence intensity of magnetic poly(*N*-isopropylacrylamide) microspheres inside cells

The mean fluorescence intensity at different drug concentrations (DMPM and FDMPM) was analyzed in breast cancer cells by flow cytometry [21]. Figure 7 shows that fluorescence intensity was higher in cells treated with FDMPM (black bar) than those treated with DMPM (white bar). The difference was statistically significant.

Cytotoxicity assay

As shown in Fig. 8, MPM and FMPM had no depressant effects on cells, whereas DMPM and FDMPM significantly suppressed SKBR-3 cells at 48 h ($P < 0.05$).

Moreover, we measured the survival rate of SKBR-3 cells at 48 h by using the trypan blue exclusion assay. Figure 9a shows the blue cells that indicate cell death. Figure 9b suggests that there is a significant difference in survival rate between DMPM-treated and FDMPM-treated cells.

Discussion

Cancer therapy is still a challenge and numerous strategies have been developed towards targeted therapy [22]. These include increasing drug concentration within the tumor tissues or cells, simplifying delivery procedures, lowering dosages for treatment, and reducing toxicity and side effects. The combination of nanotechnology and medicine improves tumor-tagged therapy. New drug delivery systems involve the receptor–ligand nanotechnology [23]. The drug and ligand are prepared in a stable system. After administration, the nanoparticles locate the target by specific interaction of its conjugated ligand with receptors. In this way, drugs contained in the nanoparticles are released to produce localized effects at diseased sites. The principle of a targeted effect is to achieve high efficiency with low toxicity. Interest in FRs for drug targeting has increased rapidly. Compared with most other ligands under investigation (e.g. monoclonal IgGs, peptide hormones, etc.), folate is smaller, less immunogenic, more stable, easier to conjugate, less expensive, and more tumor specific. All these enhance its effectiveness in cancer therapy [24]. Furthermore, folate conjugates tested to date do not have apparent toxicity [25]. Thus, folate-targeted drugs have significant potential for clinical applications. Our RT-PCR results show that the FR gene

was expressed in SKBR-3 cells, which is in agreement with western blot results from Jhaveri *et al.* [26].

Internalization of nanodrugs by cancer cells can be facilitated through specific ligand–receptor interaction [27]. After conjugation to macromolecules, folate retains its ligand-binding property. pH-sensitive amphiphilic *N*-isopropylacrylamide copolymers facilitate transfer of liposomal content from the endosomes/lysosomes to the cytoplasm [28]. Therefore, by combining the tumor-targeting ability of folate with the unique physicochemical properties of copolymers, we can generate highly efficient liposomal systems for cytoplasmic delivery of a variety of active compounds [29]. In this study, we synthesized FDMPMs. FDMPMs were clearly observed within FR-positive SKBR-3 cells under light or confocal microscopes even after the cells were digested, suggesting that FDMPM was internalized by cells. Using flow cytometry, we assessed intracellular DMPM and FDMPM concentrations after internalization. We found no difference between fluorescence intensity in SKBR-3 cells at low concentrations of DMPM and FDMPM. However, the difference became significant as the drug concentration increased. These results prove that nanotechnology can increase the concentration of a therapeutic agent in cancer cells by improving delivery.

When incubated with FR-positive cells at 37°C, the drug-carrying PMs were captured, internalized, and deflated rapidly. Consequently, the carried drug was released quickly by extrusion resulting in high local concentration, which enhanced cancer cell destruction. This property of nanoparticles has also been observed *in vivo*. After intake of the ZnPcS-loaded nanoparticles by zebra fish at an optimal living temperature (28°C), the nanoparticles aggregated in the intestinal tract. After heating to 37°C for 30 min, the fluorescence of ZnPcS became diffuse, demonstrating a release of ZnPcS from nanoparticles in the fish intestinal tract. The results support the suggestion that nanoparticles have the potential for drug delivery *in vivo* [30]. However, when drug-containing PMs were injected intravenously at 37°C, the PM volume deflated and rapidly released the carried drugs. To produce effective anticancer effects, chemotherapeutic concentrations need to be high in tumor tissue for a longer period of time to affect all phases of the cell cycle. If the LCST is raised, the PM will shrink more slowly and the drugs will be released gradually, thus drug delivery could be controlled and optimized. Therefore, the velocity and extent of the volume change in polymers is a critical future research area.

Conclusion

In short, our studies show that FDMPM was localized inside cancer cells, and DOX was released as it deflated. FR-positive breast cancer cells had more rapid internalization for FDMPM than DMPM. Furthermore, our cell toxicity assessment showed that cell survival rate was higher for DMPM than FDMPM, confirming that folate-bearing agents are more effective for treating FR-positive cancer cells.

Acknowledgements

This study was supported by the National Science Foundation for Distinguished Young Scholars of China (50525310), Shanghai Leading Academic Discipline Project (B113) and Shanghai Technology Innovation Project(0852nm04400).

References

1 Moore M. Masking of fluorescence by tetrachloroparabenzoquinone (spergon). *AMA Arch Dermatol Syphilol* 1952; **66**:621–623.
2 Carter SK. Adriamycin. *J Natl Cancer Inst* 1975; **55**:1265–1274.
3 Filyak Y, Filyak O, Souchelnytskyi S. Doxorubicin inhibits TGF-beta signaling in human lung carcinoma A549 cells. *Eur J Pharmacol* 2008; **590**:67–73.
4 Gewirtz DA. A critical evaluation of the mechanisms of action proposed for the antitumor effects of the anthracycline antibiotics adriamycin and daunorubicin. *Biochem Pharmacol* 1999; **57**:727–741.
5 Kost J, Langer R. Responsive polymer delivery systems. *Adv Drug Deliv Rev* 2001; **46**:125–148.
6 Dai X, Yue Z, Eccleston ME, Swartling J, Slater NK, Kaminski CF. Fluorescence intensity and lifetime imaging of free and micellar-encapsulated doxorubicin in living cells. *Nanomedicine* 2008; **4**:49–56.
7 Chu LY, Park SH, Yamaguchi T, Nakao S. Preparation of micron-sized monodispersed thermoresponsive core-shell microcapsules. *Langmuir* 2002; **18**:1856–1864.
8 Ibarz G, Dahne L, Donath E, Mohwald H. Smart micro- and nanocontainers for storage, transport, and release. *Adv Mater* 2001; **13**:1324–1327.
9 Zelikin AN, Becker AL, Johnston APR, Wark KL, Turatti F, Caruso F. A general approach for DNA encapsulation in degradable polymer miocrocapsules. *ACS Nano* 2007; **1**:63–69.
10 Twaites BR, Alarcon CD, Cunliffe D, Lavigne M, Pennadam S. Thermo and pH responsive polymers as gene delivery vectors: effect of polymer architecture on DNA complexation in vitro. *J Control Release* 2004; **97**:551–566.
11 Feil H, Bae YH, Jan FJ, Kim SW. Effect of comonomer hydrophilicity and ionization on the lower critical solution temperature of N-isopropylacrylamide copolymers. *Macromolecules* 1993; **26**:2496–2500.
12 Bucak S, Jones DA, Laibinis PE, Hatton TA. Protein separations using colloidal magnetic nanoparticles. *Biotechnol Prog* 2003; **19**:477–484.
13 Bulte JWM, Ouglas TD, Witwer B, Zhang SC. Magnetodendrimers allow endosomal magnetic labeling and in vivo tracking of stem cells. *Nat Biotechnol* 2001; **19**:1141–1147.
14 Doyle PS, Bibette J, Bancaud A, Viovy JL. Self-assembled magnetic matrices for DNA separation chips. *Science* 2002; **295**:2237.
15 Garin-Chesa P, Campbell I, Saigo PE, Lewis JL, Old LJ, Rettig WJ. Trophoblast and ovarian cancer antigen LK26 Sensitivity and specificity in immunopathology and molecular identification as a folate-binding protein. *Am J Pathol* 1993; **142**:557–567.
16 Ross JF, Chaudhuri PK, Ratnam M. Differential regulation of folate receptor isoforms in normal and malignant tissues in vivo and in established cell lines. Physiologic and clinical implications. *Cancer* 1994; **73**:2432–2443.
17 Liu SQ, Wiradharma N, Gao SJ, Tong YW, Yang YY. Bio-functional micelles self-assembled from a folate-conjugated block copolymer for targeted intracellular delivery of anticancer drugs. *Biomaterials* 2007; **28**:1423–1433.
18 You J, Li X, de Cui F. Folate-conjugated polymer micelles for active targeting to cancer cells: preparation, in vitro evaluation of targeting ability and cytotoxicity. *Nanotechnology* 2008; **19**:45102–45110.
19 Soppimath KS, Liu LH, Seow WY, Liu SQ, Powell R. Multifunctional core/shell nanoparticles self-assembled from pH-induced thermosensitive polymers for targeted intracellular anticancer drug delivery. *Adv Funct Mater* 2007; **17**:355.
20 Mohapatra S, Mallick SK, Maiti TK, Ghosh SK, Pramanik P. Synthesis of highly stable folic acid conjugated magnetite nanoparticles for targeting cancer cells. *Nanotechnology* 2007; **18**:385102.
21 Lanklma J, Dekker H, Luque RF. Doxorubicin gradients in human breast cancer. *Clin Cancer Res* 1999; **5**:1703–1707.

22 Roche AC, Barzilay M, Midoux P. Sugar-specific endocytosis of glycoproteins by lewis lung-carcinoma cells. *J Cell Biochem* 1983; **22**:131–140.
23 Severin Ye S, Muizhnek Ye L, Severin Ye S. Targeted delivery of antitumor drugs by protein vectors. *Vestnik Rossiiskoi Akademii Meditsinskikh Nauk* 1999; **5**:22–28.
24 Hilgenbrink AR, Low PS. Folate receptor-mediated drug targeting: From therapeutics to diagnostics. *Pharm Sci* 2005; **94**:2135–2146.
25 Low PS, Antony AC. Folate receptor-targeted drugs for cancer and inflammatory diseases. *Adv Drug Deliv Rev* 2004; **56**:1055–1058.
26 Jhaveri MS, Rait AS, Chung KN. Antisense oligonucleotides targeted to the human alpha folate receptor inhibit breast cancer cell growth and sensitize the cells to doxorubicin treatment. *Mol Cancer Ther* 2004; **3**:1505–1512.
27 Mori T. Cancer-specific ligands identified from screening of peptide-display libraries. *Curr Pharm Des* 2004; **10**:2335–2343.
28 Francis MF, Dhara G, Winnik FM, Leroux JC. In vitro evaluation of pH-sensitive polymer/niosome complexes. *Biomacromolecules* 2001; **2**:741–749.
29 Dubé D, Francis M, Leroux JC, Winnik FM. Preparation and tumor cell uptake of poly(N-isopropylacrylamide) folate conjugates. *Bioconjug Chem* 2002; **13**:685–692.
30 He J, Chen JY, Wang P. Poly(N-isopropylacrylamide)-coated thermo-responsive nanoparticles for controlled delivery of sulfonated Zn-phthalocyanine in Chinese hamster ovary cells in vitro and zebra fish in vivo. *Nanotechnology* 2007; **18**:415101.